

# **Seismicity in Pennsylvania from February 2013 to June 2015**

## **Report submitted to the State Geologist and Director of the Bureau of Topographic and Geologic Survey, Department of Conservation and Natural Resources**

Andrew Nyblade and Kyle Homman, Department of Geosciences, Pennsylvania State University, University Park, PA 16802 email: [aan2@psu.edu](mailto:aan2@psu.edu)

September 23, 2016

### **Summary**

Broadband seismic data from 101 stations operating within and surrounding Pennsylvania from February 2013 to June 2015 have been used to locate seismic events and estimate magnitudes. The data come from five seismic networks, with most of the data provided by two temporary networks, the USArray Transportable Array (TA) network and the PASEIS network. Event locations and magnitudes for 1,761 events were obtained and assembled into a catalog that is provided with this report. 1,544 of the events are within Pennsylvania. Event magnitudes, determined using a local magnitude scale ( $M_L$ ) for the eastern U.S., range between 0.7 and 3.0, with an average magnitude of 1.8. The magnitude of completeness ( $M_C$ ) for the catalog is  $M_L$  1.8 and the b-value is 3.1. 1,530 of the events in Pennsylvania can be correlated with mining activity based on the proximity of events to mines or quarries, event origin times on weekdays during working hours, and a number of waveform characteristics. For the other 14 events, there is no correlation in time or space with gas drilling activity or waste water disposal, and therefore these events are most probably natural earthquakes.

### **Introduction**

This report is provided in fulfillment of a contract from the Bureau of Topographic and Geologic Survey (BTGS) to monitor and locate seismicity in Pennsylvania during the time period in which the EarthScope USArray Transportable Array (TA) (<http://www.usarray.org>) seismic network was deployed in Pennsylvania. The TA seismic stations were installed in Pennsylvania starting in December 2012, and the demobilization of the last station occurred in May 2015. The BTGS provided funding to Penn State to (1) densify the TA network with temporary seismic stations (the PASEIS network) beginning in early 2013, and (2) to use data from all available seismic stations within and surrounding Pennsylvania to locate seismic events and construct a catalog of event locations and magnitudes. The initial agreement with the BTGS was to operate the PASEIS network from early 2013 through December 2014 and to provide a catalog of seismic events through December 2014. However, many of the TA stations were not removed until mid-2015, and consequently the project was extended so that seismic events that occurred between January and June 2015 could be added to the catalog. In addition to supporting the installation and operation of the temporary PASEIS stations, the BTGS has provided funding to Penn State for a number of years to operate a network of permanent seismic stations (also referred to as the PASEIS network). Data from the permanent PASEIS stations, as

well as from several other permanent stations within and adjacent to Pennsylvania have also been used in this study.

To put the findings of this study in context, Figure 1 shows seismic events within and surrounding Pennsylvania in the U.S. Geological Survey (USGS) earthquake catalog from 1970 to 2015. At the end of this report we also briefly review the findings from Homman (2015), who analyzed event locations, origin times and waveform characteristics to determine the most likely source of each event in the catalog.

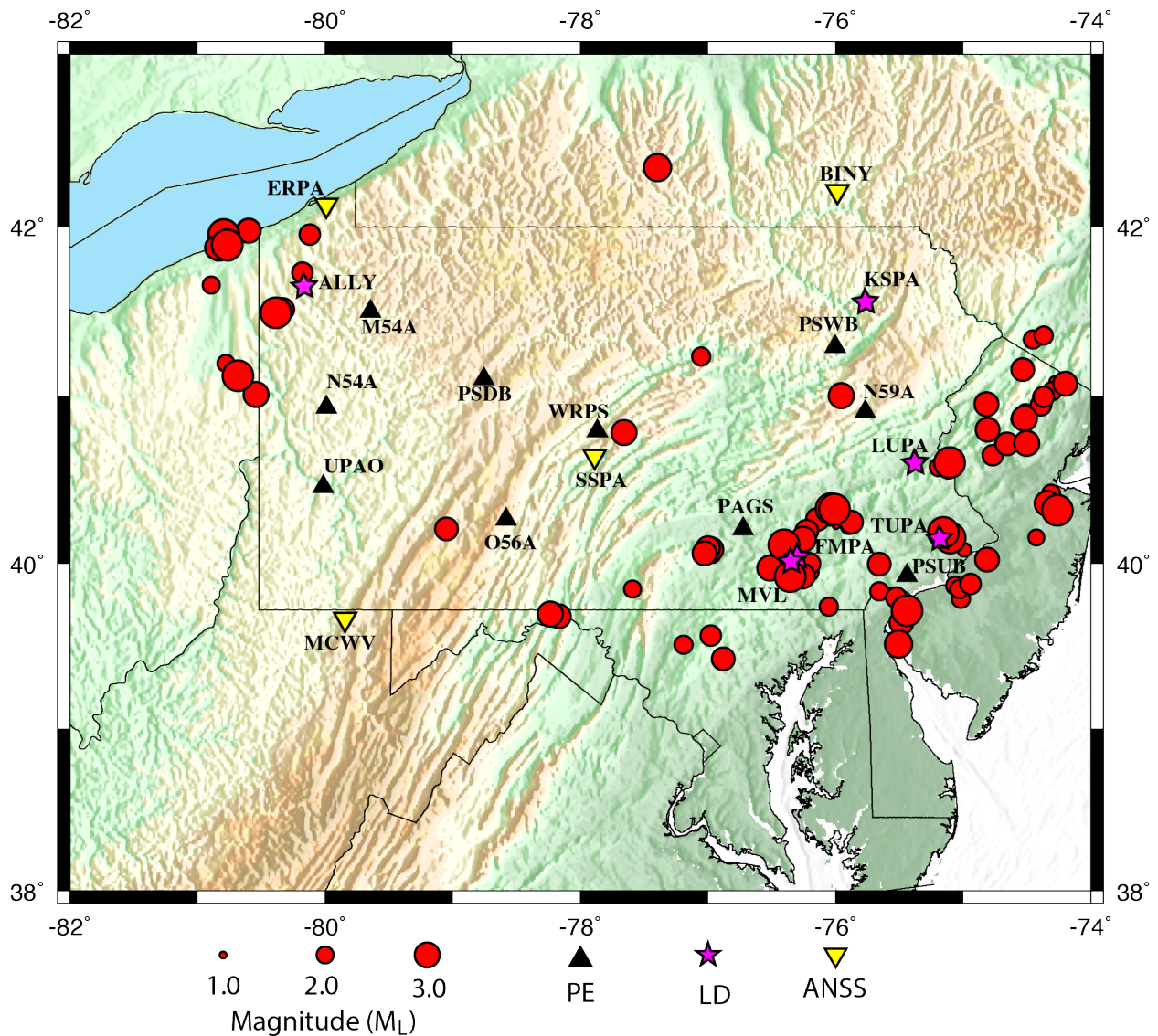


Figure 1: Topographic map showing earthquakes within and surrounding Pennsylvania between 1970 and 2015 from the USGS catalog (red circles). Permanent seismic stations providing open access data within and surrounding Pennsylvania are also shown. See text for explanation of the network abbreviations PE, LD and ANSS.

### Seismic Networks and Data

The data used in this study comes from 101 broadband stations belonging to five seismic networks that were in operation over the time period of the study (February 2013 – June 2015). Figure 2 shows the station locations, and a complete listing of the stations, together with station instrumentation and network codes, is given in Appendix 1. The ensemble of stations provides a station spacing of ~30 to 50 km across Pennsylvania. Details about the stations beyond what is summarized below can be obtained from the Incorporated Research Institutions for Seismology (IRIS) data management center’s metadata aggregator (<http://ds.iris.edu/mda/network> code). All of the data used in this study are archived at the IRIS data management center (<http://ds.iris.edu/ds/nodes/dmc/>) and are openly available.

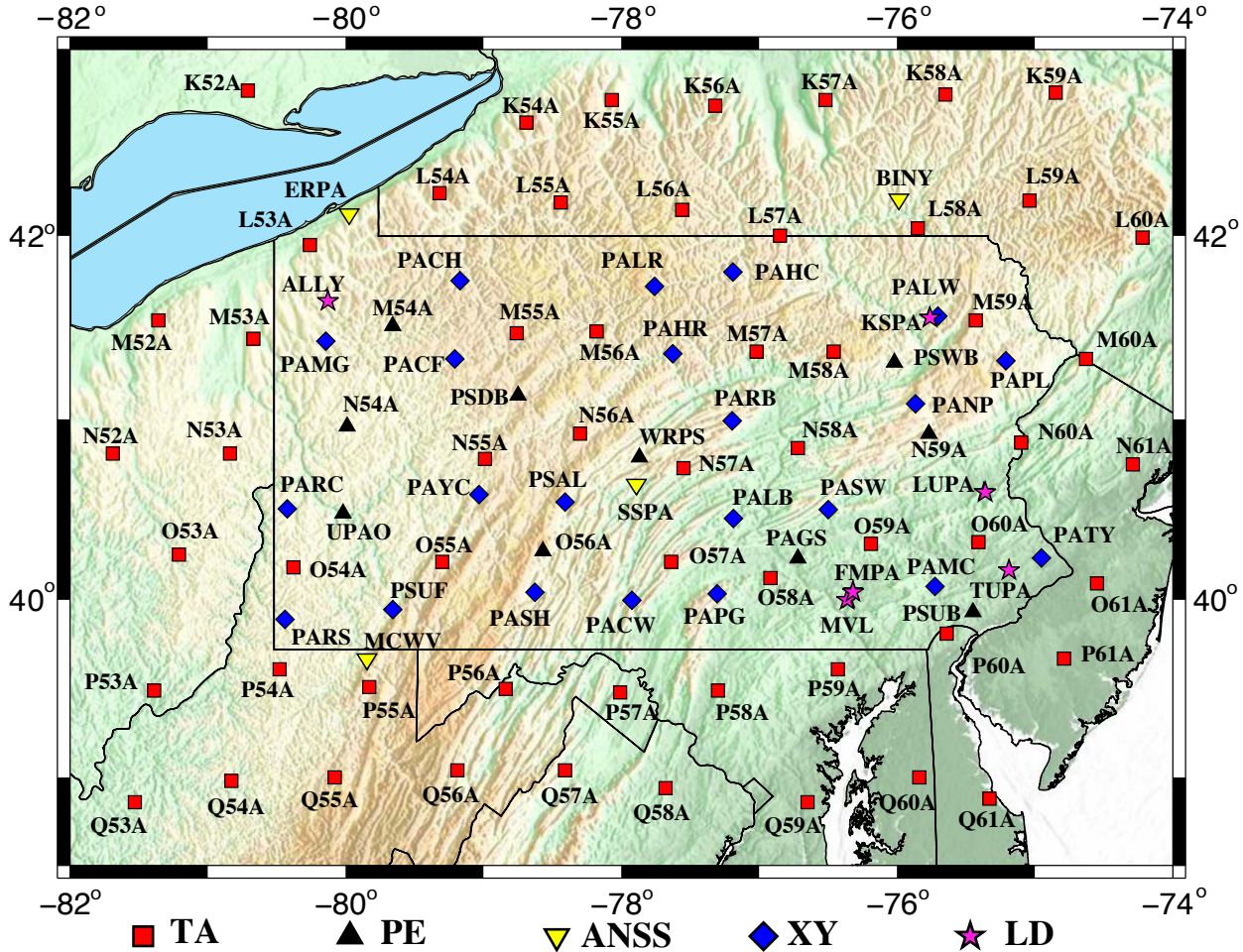


Figure 2: Topographic map showing seismic stations within and adjacent to Pennsylvania used in this study. See text for explanation of the network abbreviations TA, PE, ANSS, XY, and LD.

#### ***Advanced National Seismic System (ANSS) (Network codes IU and US):***

The Advanced National Seismic System (ANSS) consists of two networks, the Global Seismographic Network (GSN) and the United States Seismic Network (USN). The GSN is operated jointly by IRIS and the USGS, and the USN is operated by the USGS. Data from four stations in the ANSS, two in Pennsylvania and two in neighboring states (Figure 2), have been used. Three of the stations (ERPA, BINY, and MCWV) belong to the USN and one station

(SSPA) belongs to the GSN. The USN stations are equipped with Streckheisen STS-2 sensors and Quanterra 330 dataloggers. Station SSPA is equipped with a Geotech KS-36000-I borehole sensor.

***Permanent PASEIS Network (Network Code PE):***

Penn State, with support from the BTGS, established a real time three-component broadband seismic network beginning in 2006 for the Commonwealth. Over a period of several years, five stations were installed and combined with an existing station (WRPS) in the Department of Geoscience at the Penn State University Park campus to create a network of permanent seismic stations. Three of the stations are located at Penn State branch campuses, one is at the University of Pittsburgh, and one is at the BTGS headquarters in Middletown. The six stations are equipped with Guralp CMG3T sensors and Guralp DM24 data loggers. In 2010, an additional four stations were added to the network by advanced purchase of USArray TA stations N54A, M54A, O56A, N59A (Figures 1 and 2).

Information about the permanent PASEIS stations can be found with two network codes. The first network code, PE, contains the six initial stations in the network. The second, \_PENN, is an IRIS virtual network that contains the six PE stations as well as the four advanced purchase TA stations for the time period of 2010-2016. Additional station information is given in Appendix 2.

***Lamont-Doherty Cooperative Seismographic Network (network code LD):***

Lamont-Doherty Earth Observatory operates a 40-station seismic network in the northeastern U.S. (Lamont-Doherty Cooperative Seismograph Network; LCSN), which is supported by the USGS. There are six LCSN stations in Pennsylvania, and data from all six have been used in this study (Figure 2). The stations are equipped either with a Guralp CMG 3ESP, a Guralp CMG 40T, or a Nanometrics Trillium 120P sensor. RefTek RT130 or Quanterra Q730 data loggers are used at these stations.

***USArray Transportable Array (network code TA):***

The majority of the stations used in this study were part of the USArray Transportable Array (TA). Data from 20 TA stations located in Pennsylvania and 43 stations in neighboring states have been used (Figure 2). The TA network started in August 2007 in the western United States and migrated eastward, reaching western Pennsylvania in late 2012. Station spacing for the TA was approximately 70 km, with the stations deployed in a grid pattern. TA stations in Pennsylvania recorded data for an average of 22.6 months. The first TA station was installed in Pennsylvania in December 2012 and the last TA station was installed in August 2013. Demobilization of the stations started in October 2014 and was completed in May 2015. The TA stations were equipped with Quanterra 330 data loggers and either Guralp CMG3T, Streckheisen STS-2, or Nanometrics Trillium 240 sensors.

***Temporary PASEIS Network (network code XY):***

In order to reduce station spacing to ~30 to 50 km and increase the level of seismic detection, deployment of temporary PASEIS stations began in early 2013. Twenty-one stations were installed between February 2013 and May 2013 and one station was installed in August 2013 (Figure 2). Twenty stations were located at Pennsylvania state parks and two stations at Penn State branch campuses. The stations were equipped with Nanometrics Compact Trillium sensors and RefTek RT130 data loggers. Stations were visited every 3-4 months for data

downloading, and the data have been archived at the IRIS data management center. Additional station information is given in Appendix 2.

### Seismic Event Catalog

To generate a seismic event catalog, data from the 101 seismic stations were used for locating events and estimating magnitudes. The Antelope Environmental Data Collection Software suite (Antelope) was used to pick P-wave arrival times and obtain initial locations. S-wave arrivals were not picked. The methods used are similar to the methods outlined in the Antelope New Users Guide (Lockridge et al., 2012), except that the automated event detection and location codes described in the Users Guide were not used.

Antelope's *dbpick* program was used to visually scan continuous waveform data from the stations. The data were filtered with a 1-5 Hz bandpass filter, and then P wave arrival times were hand picked to within 0.1 s. Preliminary hypocenters were found by using Antelope's *dblocs2* program and the IASP91 (Kennett and Engdahl, 1991) velocity model. *Dblocs2* uses an iterative non-linear inverse technique where the least-squares inversion employs a singular value decomposition method (Bratt and Bache, 1988). To further refine event locations, the events were relocated using the HYPOELLIPSE (Lahr, 1989; Lahr, 1999) program and a velocity model for Pennsylvania modified from Katz (1955) (Table 1). HYPOELLIPSE uses Geiger's method (Geiger, 1912; Lahr, 1989; Lahr, 1999), which is an iterative least-squares method, to determine hypocenter location. Local magnitudes ( $M_R$ ) were determined using Antelope's *dbevproc* program, which follows Richter's (1935) method for southern California and uses the largest amplitude on the three-component data. To obtain magnitude estimates using attenuation parameters that are more appropriate for the eastern U.S., a local magnitude ( $M_L$ ) was computed using the magnitude equation from Kim (1998). Both  $M_R$  and  $M_L$  magnitudes are provided in the event catalog.

Locations were obtained using a minimum of four P-wave arrival times, and the average number used was 11. Residuals for P-wave travel times were generally less than 1s, although a few travel times had residuals between 1 and 2.5 seconds. The average overall root mean square (RMS) travel time residual for the catalog is 0.5 seconds.

Table 1: Velocity model used for event location with the HYPOELLIPSE code

| Layer | P-wave Velocity (km/s) | Depth of interface (km) | Vp/Vs ratio |
|-------|------------------------|-------------------------|-------------|
| 1     | 6.0                    | 0.0                     | 1.74        |
| 2     | 6.3                    | 10.0                    | 1.74        |
| 3     | 6.6                    | 20.0                    | 1.74        |
| 4     | 6.9                    | 30.0                    | 1.74        |
| 5     | 8.1                    | 37.0                    | 1.74        |

The catalog contains details of seismic event locations and magnitudes. Event origin time information is given to within 0.01 seconds. An azimuthal gap is reported, which is the largest number of degrees azimuthally between adjacent stations. Generally, a smaller azimuthal gap corresponds to a more reliable event location. The RMS (root mean square) value listed in

the catalog is the overall RMS residual of the travel time picks used in the location. An error ellipse provides a minimum estimate of the event location uncertainty. The error ellipse is computed using a 68% confidence bound and one degree of freedom.

## Results

The catalog (Excel file attached to this report) contains locations and magnitudes for 1,761 events, 1,544 of which are located within Pennsylvania (Figure 3). Events outside of the state are mostly situated near the border and were located to verify that they did not fall within the state boundaries.

The epicentral locations for all events in Pennsylvania are well constrained, as indicated by the average formal horizontal error ellipse axis of  $< 0.5$  km. In addition, depths for 1105 of the events are fairly well constrained, with an average depth uncertainty of 1.3 km. However, the remaining events in the catalog have depth uncertainties of  $> 5$  km. There is a trade-off between source depth and origin time, and therefore it is possible that the origin time of events with poorly constrained depths may be inaccurate. The depth distribution for the 1105 events with well-constrained source depths is illustrated in Figure 4.

The average local magnitude ( $M_L$ ) is 1.8 and the magnitude range is 0.7 to 3.0 (Figure 5). Using the maximum curvature (MAXC) technique of Wiemer and Wyss (2000) and the Gutenberg-Richter plot (Figure 6), the magnitude of completeness ( $M_C$ ) of the catalog is estimated to be  $M_L$  1.8. The b-value obtained for the catalog is 3.1, which is much higher than the expected b-value of 1.0 for natural earthquakes. b-values for blasting events are typically greater than 1.5 (Wiemer and Baer, 2000), which suggests that the catalog is dominated by mining-related seismic events. Origin times for the seismic events occur primarily between 12:00 and 22:00 UTC (8 am and 6 pm EST) (Figures 7 and 8), and the majority of the events occur Monday through Friday, with significantly fewer events on weekend days (Figure 9).

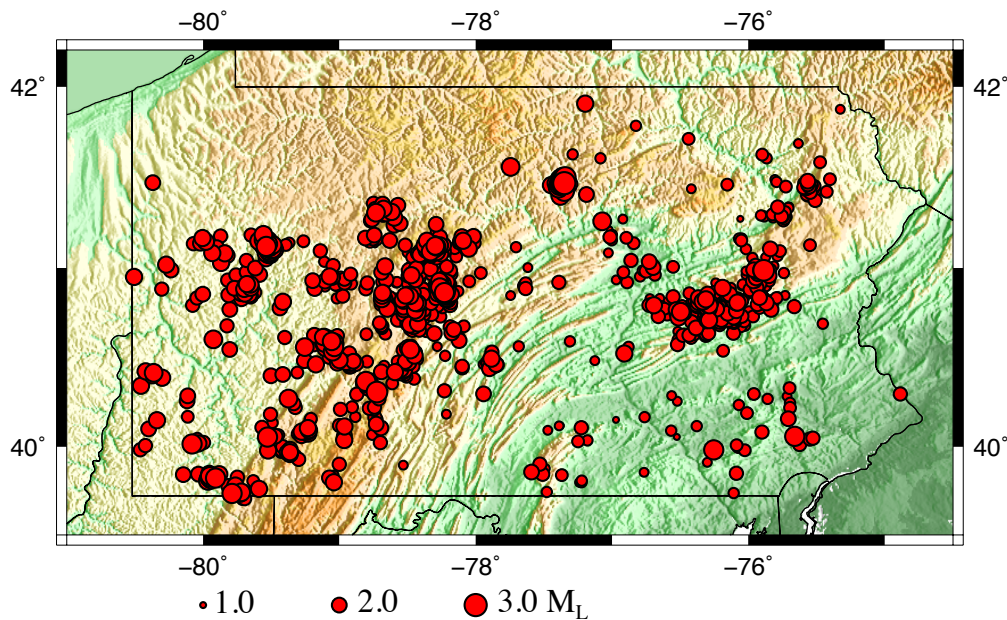


Figure 3: Seismic events (red circles) in Pennsylvania between February 2013 and June 2015.

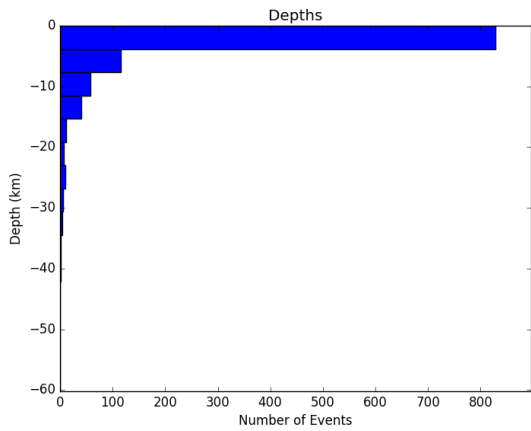


Figure 4. Depth distribution of seismic events with well constrained source depths.

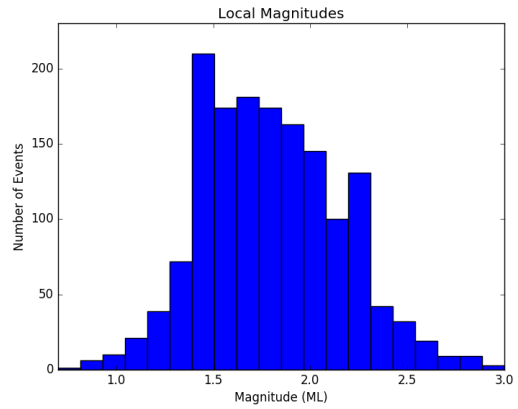


Figure 5. Magnitude distribution of seismic events.

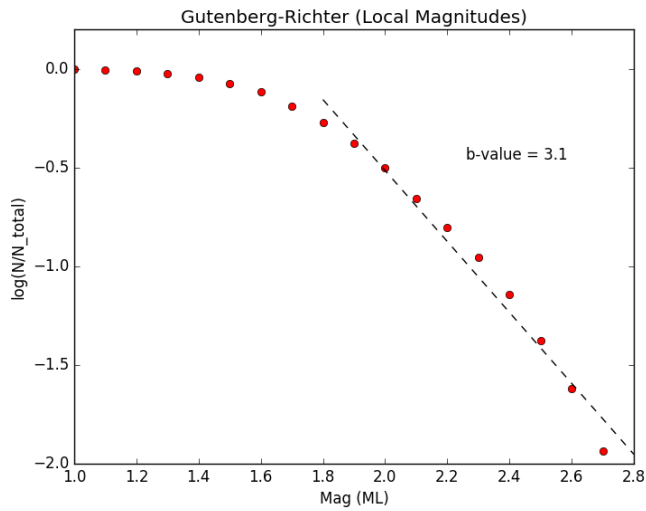


Figure 6. Gutenberg-Richter plot for events in Pennsylvania. The slope of the dashed line gives a b-value of 3.1.

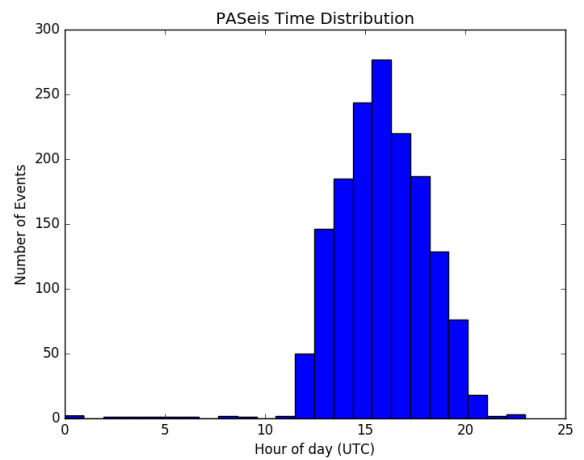


Figure 7. Histogram showing the distribution of seismic event origin times by hour.

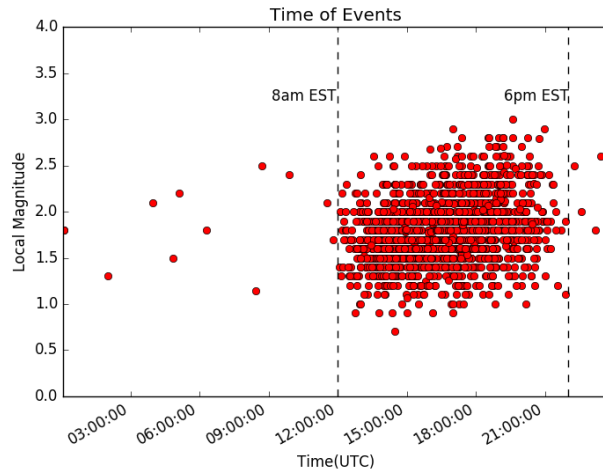


Figure 8. Scatter plot showing the distribution of seismic origin times by hour versus local magnitude.

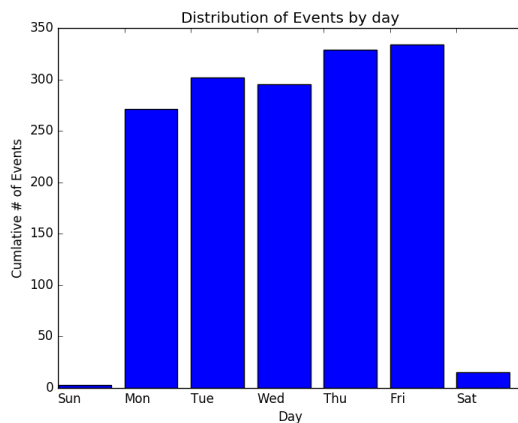


Figure 9. Histogram showing distribution of event origin times by day.

### Comparison with the USGS Catalog

For the time period of this study, the USGS seismic event catalog contains six earthquakes and one mine blast. Locations and magnitudes are comparable between the two catalogs for these events. The USGS does not routinely report seismic event information for mine blasts.

### Review of seismic sources from Homman’s M.S. Thesis

The event origin times show a strong bias towards events on weekdays and working hours (Figures 7, 8 and 9), and as mentioned above, the Gutenberg-Richter analysis yielded a b-value of 3.1. The timing distribution and b-value combined suggest that the seismicity catalog is dominated by mine blasts, but there also could be events from other sources contained in the catalog.

An investigation of seismicity sources was conducted by Homman (2015) to identify the nature of seismic events in the catalog. To associate events with mining activity, mine locations were gathered from the Pennsylvania Department of Environmental Protection open reports on bituminous coal, anthracite coal, and industrial minerals production. A strong visual correlation between event and mine locations was found. The correlation is particularly evident between the locations of bituminous and anthracite coal mines with seismic events, but also between some industrial mineral quarries and seismic events.



Homman (2015) then classified events based on criteria used by the USGS for identifying seismicity caused by blasting, including frequency characteristics of the data. By combining the results of this classification with the location and timing of events, Homman (2015) showed that only a handful of events in the catalog were probably not related to mining activity. P-wave and S-wave arrival times for the non-mining events were repicked using 1-10 Hz bandpass filtered data and relocated using the Pennsylvania velocity model (Table 1) and the HYPOELLIPSE code. The refined event locations and origin times were then examined to determine if there were spatial and temporal correlations with natural gas exploration activity or waste water disposal. No correlation was found and therefore Homman (2015) concluded that there is little, if any, evidence for seismic events in the catalog caused by hydraulic fracturing or waste water injection. The only other likely source for the non-mining related events is natural seismicity, and therefore Homman (2015) further concluded that the events are most probably earthquakes. A table and map of the non-mining events are provided below.

Table 2. Non-mining events in the catalog.

| YRMMDD   | Hr:Min | Sec   | Lat. (deg) | Lon. (deg) | Depth (km) | M <sub>R</sub> | M <sub>L</sub> |
|----------|--------|-------|------------|------------|------------|----------------|----------------|
| 20130219 | 9:53   | 3.24  | 41.2587    | -77.0722   | 10.6       | 2.3            | 2.4            |
| 20130703 | 5:04   | 24.54 | 40.2207    | -79.3243   | 1.1        | 1.7            | 1.8            |
| 20130703 | 5:06   | 16.28 | 40.2422    | -79.3353   | 0.0        | 1.7            | 1.8            |
| 20130716 | 3:58   | 9.51  | 39.8563    | -77.5902   | 0.0        | 1.9            | 2.1            |
| 20130718 | 4:51   | 49.32 | 39.8604    | -77.5921   | 0.1        | 1.7            | 1.5            |
| 20130824 | 5:07   | 26.89 | 40.1491    | -80.3384   | 0.1        | 2.2            | 2.2            |
| 20140109 | 2:02   | 38.26 | 39.9116    | -76.3014   | 5.8        | 1.5            | 1.3            |
| 20140209 | 22:34  | 4.23  | 41.4734    | -80.3687   | 4.3        | 2.0            | 2.0            |
| 20140305 | 6:18   | 9.08  | 39.9826    | -80.4600   | 0.0        | 1.9            | 1.8            |
| 20140729 | 20:12  | 7.27  | 40.4432    | -78.0994   | 27.8       | 2.0            | 1.8            |
| 20140905 | 20:00  | 10.85 | 40.2554    | -76.5222   | 0.0        | 1.3            | 1.2            |
| 20140921 | 8:27   | 49.99 | 40.1509    | -76.9719   | 14.4       | 1.3            | 1.1            |
| 20150125 | 23:25  | 10.68 | 40.058     | -75.6603   | 0.0        | 2.9            | 2.6            |
| 20150429 | 8:42   | 58.76 | 40.2708    | -79.3741   | 0.8        | 2.7            | 2.5            |

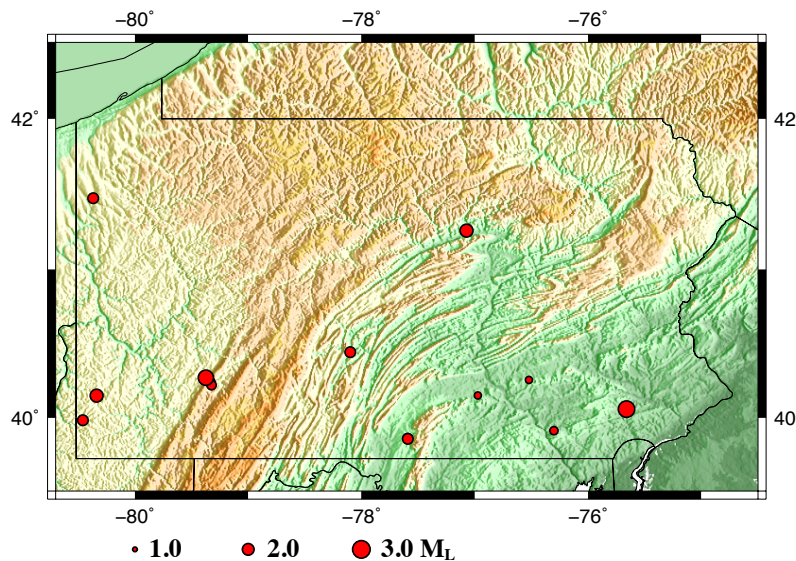


Figure 10. Map showing location of non-mining events.

## References

- Bratt, S. R., and T. C. Bache, 1988, Locating events with a sparse network of regional arrays, *Bulletin of the Seismological Society of America*, 78, 780-798.
- Geiger, L., 1912, Probability method for the determination of earthquake epicenters from the arrival time only (translated from Geiger's 1910 German article), *Bulletin of St. Louis University*, 8, 56-71.
- Homman, K., 2015, Seismicity in Pennsylvania, M.S. Thesis, The Pennsylvania State University, pp. 128.
- Kennett, B. L. N., and E. R. Engdahl, 1991, Traveltimes for Global Earthquake Locations and Phase Identification, *Geophysical Journal International*, 122, 429-465.
- Katz, S., 1955, Seismic study of crustal structure in Pennsylvania and New York, *Bulletin of the Seismological Society of America*, 45, 303-325.
- Kim, W., 1998, The ML Scale in Eastern North America, *Bulletin of the Seismological Society of America*, 88.4, 935-951.
- Lahr, J., 1989, HYPOELLIPSE/version 2.0: A Computer Program for Determining Local Earthquake Hypocentral Parameters, Magnitude, and First Motion Pattern, *US Geological Survey, Open-File Report OF 89-0116*.
- Lahr, J., 1999, HYPOELLIPSE: A Computer Program for Determining Local Earthquake Hypocentral Parameters, Magnitude, and First Motion Pattern (Y2K compliant version). *US Geological Survey, Open-File Report OF 99-0023*.
- Lockridge, J. S., M. J. Fouch, and J. R. Arrowsmith, 2012, Seismicity Within Arizona during the Deployment of the EarthScope USArray Transportable Array, *Bulletin of the Seismological Society of America*, 102.4, 1850–1863.
- Richter, C.F., 1935, An Instrumental Earthquake Magnitude Scale, *Bulletin of the Seismological Society of America*, 25, 1-32.
- Wiemer, S., 2000, Mapping And Removing Quarry Blast Events from Seismicity Catalogs, *Bulletin of the Seismological Society of America*, 90.2, 525–530.
- Wiemer, S., and M. Wyss, 2000, Minimum magnitude of complete reporting in Earthquake Catalogs: Examples from Alaska, the Western United States, and Japan, *Bulletin of the Seismological Society of America*, 90, 859-869.

**Appendix 1: Seismic stations used in this study.**

| <b>Station</b> | <b>Lat.</b> | <b>Lon.</b> | <b>Network</b> | <b>Network Code</b> | <b>Sensor</b>      | <b>Datalogger</b> |
|----------------|-------------|-------------|----------------|---------------------|--------------------|-------------------|
| K52A           | 42.78       | -80.71      | TA             | TA                  | Streckheisen STS-2 | Quanterra 330     |
| K54A           | 42.61       | -78.69      | TA             | TA                  | Streckheisen STS-2 | Quanterra 330     |
| K55A           | 42.73       | -78.07      | TA             | TA                  | Streckheisen STS-2 | Quanterra 330     |
| K56A           | 42.70       | -77.32      | TA             | TA                  | Guralp CMG3T       | Quanterra 330     |
| K57A           | 42.73       | -76.52      | TA             | TA                  | Streckheisen STS-2 | Quanterra 330     |
| K58A           | 42.76       | -75.65      | TA             | TA                  | Guralp CMG3T       | Quanterra 330     |
| K59A           | 42.77       | -74.85      | TA             | TA                  | Streckheisen STS-2 | Quanterra 330     |
| K60A           | 42.62       | -73.89      | TA             | TA                  | Streckheisen STS-2 | Quanterra 330     |
| L53A           | 41.95       | -80.26      | TA             | TA                  | Trillium 240       | Quanterra 330     |
| L54A           | 42.23       | -79.32      | TA             | TA                  | Trillium 240       | Quanterra 330     |
| L55A           | 42.18       | -78.44      | TA             | TA                  | Trillium 240       | Quanterra 330     |
| L56A           | 42.14       | -77.56      | TA             | TA                  | Guralp CMG3T       | Quanterra 330     |
| L57A           | 42.00       | -76.85      | TA             | TA                  | Streckheisen STS-2 | Quanterra 330     |
| L58A           | 42.04       | -75.85      | TA             | TA                  | Guralp CMG3T       | Quanterra 330     |
| L59A           | 42.19       | -75.04      | TA             | TA                  | Streckheisen STS-2 | Quanterra 330     |
| L60A           | 41.99       | -74.22      | TA             | TA                  | Trillium 240       | Quanterra 330     |
| M52A           | 41.54       | -81.36      | TA             | TA                  | Trillium 240       | Quanterra 330     |
| M53A           | 41.44       | -80.67      | TA             | TA                  | Trillium 240       | Quanterra 330     |
| M54A           | 41.51       | -79.66      | TA             | TA                  | Guralp CMG3T       | Quanterra 330     |
| M55A           | 41.47       | -78.76      | TA             | TA                  | Streckheisen STS-2 | Quanterra 330     |
| M56A           | 41.48       | -78.18      | TA             | TA                  | Streckheisen STS-2 | Quanterra 330     |
| M57A           | 41.37       | -77.02      | TA             | TA                  | Streckheisen STS-2 | Quanterra 330     |
| M58A           | 41.37       | -76.46      | TA             | TA                  | Guralp CMG3T       | Quanterra 330     |
| M59A           | 41.54       | -75.43      | TA             | TA                  | Streckheisen STS-2 | Quanterra 330     |
| M60A           | 41.33       | -74.63      | TA             | TA                  | Streckheisen STS-2 | Quanterra 330     |
| M61A           | 41.31       | -73.77      | TA             | TA                  | Trillium 240       | Quanterra 330     |
| N52A           | 40.81       | -81.69      | TA             | TA                  | Guralp CMG3T       | Quanterra 330     |
| N53A           | 40.81       | -80.84      | TA             | TA                  | Trillium 240       | Quanterra 330     |
| N54A           | 40.96       | -79.99      | TA             | TA                  | Guralp CMG3T       | Quanterra 330     |
| N55A           | 40.78       | -78.99      | TA             | TA                  | Trillium 240       | Quanterra 330     |
| N56A           | 40.92       | -78.30      | TA             | TA                  | Streckheisen STS-2 | Quanterra 330     |
| N57A           | 40.73       | -77.55      | TA             | TA                  | Streckheisen STS-2 | Quanterra 330     |
| N58A           | 40.84       | -76.72      | TA             | TA                  | Guralp CMG3T       | Quanterra 330     |
| N59A           | 40.92       | -75.77      | TA             | TA                  | Guralp CMG3T       | Quanterra 330     |

|      |       |        |        |    |                                       |               |
|------|-------|--------|--------|----|---------------------------------------|---------------|
| N60A | 40.87 | -75.10 | TA     | TA | Streckheisen STS-2                    | Quanterra 330 |
| N61A | 40.75 | -74.29 | TA     | TA | Trillium 240                          | Quanterra 330 |
| O53A | 40.25 | -81.21 | TA     | TA | Streckheisen STS-2                    | Quanterra 330 |
| O54A | 40.18 | -80.38 | TA     | TA | Streckheisen STS-2                    | Quanterra 330 |
| O55A | 40.21 | -79.30 | TA     | TA | Streckheisen STS-2                    | Quanterra 330 |
| O56A | 40.27 | -78.57 | TA     | TA | Guralp CMG3T                          | Quanterra 330 |
| O57A | 40.21 | -77.64 | TA     | TA | Streckheisen STS-2                    | Quanterra 330 |
| O58A | 40.12 | -76.92 | TA     | TA | Streckheisen STS-2                    | Quanterra 330 |
| O59A | 40.31 | -76.19 | TA     | TA | Trillium 240                          | Quanterra 330 |
| O60A | 40.32 | -75.41 | TA     | TA | Streckheisen STS-2                    | Quanterra 330 |
| O61A | 40.09 | -74.55 | TA     | TA | Trillium 240                          | Quanterra 330 |
| P53A | 39.49 | -81.39 | TA     | TA | Guralp CMG3T                          | Quanterra 330 |
| P54A | 39.61 | -80.48 | TA     | TA | Streckheisen STS-2                    | Quanterra 330 |
| P55A | 39.51 | -79.83 | TA     | TA | Streckheisen STS-2                    | Quanterra 330 |
| P56A | 39.50 | -78.84 | TA     | TA | Trillium 240                          | Quanterra 330 |
| P57A | 39.48 | -78.01 | TA     | TA | Streckheisen STS-2                    | Quanterra 330 |
|      |       |        |        |    | Guralp<br>CMG3T/Streckheisen<br>STS-2 |               |
| P58A | 39.49 | -77.30 | TA     | TA |                                       | Quanterra 330 |
| P59A | 39.61 | -76.43 | TA     | TA | Trillium 240                          | Quanterra 330 |
| P60A | 39.81 | -75.64 | TA     | TA | Streckheisen STS-2                    | Quanterra 330 |
| P61A | 39.67 | -74.79 | TA     | TA | Trillium 240                          | Quanterra 330 |
| Q53A | 38.86 | -81.53 | TA     | TA | Streckheisen STS-2                    | Quanterra 330 |
| Q54A | 38.98 | -80.83 | TA     | TA | Streckheisen STS-2                    | Quanterra 330 |
| Q55A | 39.00 | -80.08 | TA     | TA | Streckheisen STS-2                    | Quanterra 330 |
|      |       |        |        |    | Streckheisen STS-<br>2/Trillium 240   |               |
| Q56A | 39.04 | -79.19 | TA     | TA |                                       | Quanterra 330 |
| Q57A | 39.04 | -78.41 | TA     | TA | Trillium 240                          | Quanterra 330 |
| Q58A | 38.94 | -77.68 | TA     | TA | Guralp CMG3T                          | Quanterra 330 |
| Q59A | 38.86 | -76.65 | TA     | TA | Streckheisen STS-2                    | Quanterra 330 |
| Q60A | 39.00 | -75.84 | TA     | TA | Trillium 240                          | Quanterra 330 |
| Q61A | 38.88 | -75.33 | TA     | TA | Trillium 240                          | Quanterra 330 |
| PARB | 40.99 | -77.20 | PASEIS | XY | Compact Trillium                      | RT130         |
| PACF | 41.33 | -79.21 | PASEIS | XY | Compact Trillium                      | RT130         |
| PARC | 40.50 | -80.42 | PASEIS | XY | Compact Trillium                      | RT130         |
| PARS | 39.89 | -80.44 | PASEIS | XY | Compact Trillium                      | RT130         |
| PACH | 41.76 | -79.17 | PASEIS | XY | Compact Trillium                      | RT130         |
| PALR | 41.73 | -77.76 | PASEIS | XY | Compact Trillium                      | RT130         |
| PASH | 40.04 | -78.63 | PASEIS | XY | Compact Trillium                      | RT130         |

|      |       |        |        |    |   |               |
|------|-------|--------|--------|----|---|---------------|
| PSUF | 39.94 | -79.66 | PASEIS | XY | Compact Trillium                            | RT130         |
| PAYC | 40.58 | -79.03 | PASEIS | XY | Compact Trillium                            | RT130         |
| PASW | 40.50 | -76.50 | PASEIS | XY | Compact Trillium                            | RT130         |
| PAHC | 41.80 | -77.19 | PASEIS | XY | Compact Trillium                            | RT130         |
| PAHR | 41.36 | -77.63 | PASEIS | XY | Compact Trillium                            | RT130         |
| PAPG | 40.03 | -77.31 | PASEIS | XY | Compact Trillium                            | RT130         |
| PACW | 40.00 | -77.92 | PASEIS | XY | Compact Trillium                            | RT130         |
| PAPL | 41.32 | -75.21 | PASEIS | XY | Compact Trillium                            | RT130         |
| PALW | 41.56 | -75.70 | PASEIS | XY | Compact Trillium                            | RT130         |
| PALB | 40.45 | -77.19 | PASEIS | XY | Compact Trillium                            | RT130         |
| PAMC | 40.07 | -75.73 | PASEIS | XY | Compact Trillium                            | RT130         |
| PAMG | 41.43 | -80.15 | PASEIS | XY | Compact Trillium                            | RT130         |
| PANP | 41.08 | -75.87 | PASEIS | XY | Compact Trillium                            | RT130         |
| PSAL | 40.54 | -78.41 | PASEIS | XY | Compact Trillium                            | RT130         |
| PATY | 40.23 | -74.95 | PASEIS | XY | Compact Trillium                            | RT130         |
| FMPA | 40.05 | -76.32 | LCSN   | LD | Guralp CMG40T                               | Q730          |
| MVL  | 40.00 | -76.35 | LCSN   | LD | Guralp CMG3ESP                              | RT130         |
| LUPA | 40.60 | -75.37 | LCSN   | LD | Trillium 120P                               | RT130         |
| ALLY | 41.65 | -80.14 | LCSN   | LD | Guralp CMG3ESP                              | RT130         |
| TUPA | 40.17 | 75.19  | LCSN   | LD | Trillium 120P                               | RT130         |
| KSPA | 41.56 | 75.77  | LCSN   | LD | Trillium 120P                               | RT130         |
| PSDB | 41.13 | -78.75 | PASEIS | PE | Guralp CMG3T                                | Guralp DM24   |
| PAGS | 40.23 | -76.72 | PASEIS | PE | Guralp CMG3T                                | Guralp DM24   |
| PSUB | 39.93 | -75.45 | PASEIS | PE | Guralp CMG3T                                | Guralp DM24   |
| PSWB | 41.31 | -76.02 | PASEIS | PE | Guralp CMG3T                                | Guralp DM24   |
| UPAO | 40.48 | -80.02 | PASEIS | PE | Guralp CMG3T                                | Guralp DM24   |
| WRPS | 40.79 | -77.87 | PASEIS | PE | Guralp CMG3T                                | Guralp DM24   |
| SSPA | 40.64 | -77.89 | GSN    | IU | Geotech KS-36000-I<br>Borehole/Trillium 240 |               |
| ERPA | 42.12 | -79.99 | USN    | US | Streckheisen STS-2                          | Quanterra 330 |
| BINY | 42.20 | -75.99 | USN    | US | Streckheisen STS-2                          | Quanterra 330 |
| MCWV | 39.66 | -79.85 | USN    | US | Streckheisen STS-2                          | Quanterra 330 |

Appendix 2. Additional PASEIS station information.

| <b>Name:</b> | <b>Lat.</b> | <b>Lon.</b> | <b>Elev. (m)</b> | <b>Network Code</b> | <b>Descriptive Location:</b>                    |
|--------------|-------------|-------------|------------------|---------------------|---|
| PACF         | 41.33       | -79.21      | 373              | XY                  | Cook Forest State Park, near park office        |
| PARB         | 40.99       | -77.20      | 490              | XY                  | RB Winter State Park                            |
| PARC         | 40.50       | -80.42      | 296              | XY                  | Raccoon Creek State Park                        |
| PARS         | 39.89       | -80.44      | 396              | XY                  | Ryerson Station State Park                      |
| PACH         | 41.76       | -79.17      | 437              | XY                  | Chapman State Park, Nature Center               |
| PALR         | 41.73       | -77.76      | 526              | XY                  | Lyman Run State Park, Park Office               |
| PASH         | 40.04       | -78.63      | 385              | XY                  | Shawnee State Park, #3 picnic area restroom     |
| PSUF         | 39.94       | -79.66      | 373              | XY                  | Penn State Fayette Campus, University House     |
| PAYC         | 40.58       | -79.03      | 427              | XY                  | Yellow Creek State Park, Near Forestry building |
| PASW         | 40.50       | -79.50      | 178              | XY                  | Swatara State Park                              |
| PAHC         | 41.80       | -77.19      | 459              | XY                  | Hills Creek State Park                          |
| PAHR         | 41.36       | -77.63      | 256              | XY                  | Hyner Run State Park, outside park office       |
| PAPG         | 40.03       | -77.31      | 259              | XY                  | Pine Grove Furnace State Park                   |
| PACW         | 40.00       | -77.92      | 375              | XY                  | Cowans Gap State Park, Nature Center            |
| PAPL         | 41.32       | -75.21      | 561              | XY                  | Promised Land State Park                        |
| PALW         | 41.56       | -75.70      | 342              | XY                  | Lackawanna State Park, Ranger Station           |
| PALB         | 40.45       | -77.19      | 177              | XY                  | Little Buffalo State Park                       |
| PAMC         | 40.07       | -75.73      | 123              | XY                  | Marsh Creek State Park                          |
| PAMG         | 41.43       | -80.15      | 384              | XY                  | MK Goddard State Park, outside park office      |
| PANP         | 41.08       | -75.87      | 360              | XY                  | Nescopeck State Park                            |
| PSAL         | 40.54       | -78.41      | 373              | XY                  | Penn State Altoona, Environmental Research bldg |
| PATY         | 40.23       | -74.95      | 64               | XY                  | Tyler State Park, outside park office           |